STATUS OF R&Ds FOR SCSS PROJECT

T. Tanaka*, Y. Asano, H. Baba, T. Bizen, Z. Chao, H. Ego, S. Eguchi, T. Fukui, S. Goto, T. Hara,
T. Inagaki, S. Inoue, T. Ishikawa, D. Iwaki, K. Kase, Y. Kawashima, H. Kimura, H. Kitamura,
S. Kojima, T. Kudo, N. Kumagai, X. Marechal, S. Matsui, H. Matsumoto, T. Ohata, K. Onoe,
Y. Otake, T. Seike, T. Shintake, K. Shirasawa, N. Shusuke, T. Takagi, S. Takahashi,
T. Takashima, K. Tamasaku, R. Tanaka, K. Togawa, R. Tsuru, M. Yabashi, S. Yoshihiro, S. Wu
SCSS Project Team, Koto 1-1-1, Mikazuki, Sayo, Hyogo 679-5148, Japan

Abstract

SCSS or "SPring-8 Compact SASE Source" is an XFEL facility proposed at the SPring-8 and aims at an angstrom laser, whose facility scale is much smaller than other XFEL facilities. R&Ds of accelerator components such as the low-emittance electron gun, high-gradient C-band accelerator, and short-period in-vacuum undulator, which enable the SCSS concept, have been carried out from 2001. Construction of a 250-MeV prototype accelerator has been started that is composed of these components. It not only examines feasibility of each accelerator component but is also expected to give perspectives for construction and operation of the XFEL facility.

INTRODUCTION

SCSS stands for "SPring-8 Compact SASE Source" and is a SASE-XFEL facility proposed to be built at the SPring-8 site [1]-[5] as shown in Fig. 1. Combination of low-emittance electron gun, high-gradient C-band accelerator, and short-period in-vacuum undulator enables to make the whole facility more compact than the other XFEL facilities under proposal or construction. For a site for the SCSS facility, we are planning on the space adjoining the 1km beamline at the SPring-8. There are 3 reasons for choosing the SPring-8 site for SCSS: 1) it would complement the light source characteristics of the current SPring-8 8GeV storage ring, 3rd generation synchrotron radiation source, 2) it would be possible to simultaneously use the synchrotron radiation from the SPring-8 storage ring and the SCSS, and 3) the site provides a bedrock foundation with enough strength to assure a stable nanometer light source.

In order to realize the SCSS concept, designing, prototyping, and testing of each accelerator component have been carried out for about 5 years. A 250-MeV prototype accelerator based on the results of these R&Ds is now being built to demonstrate the technologies necessary for the concept of the SCSS before starting construction of the XFEL facility. The expected machine parameters for the prototype accelerator and XFEL facility are summarized in Table 1.

In this paper, details of the prototype accelerator are presented together with the results of the R&Ds of the accelerator component.
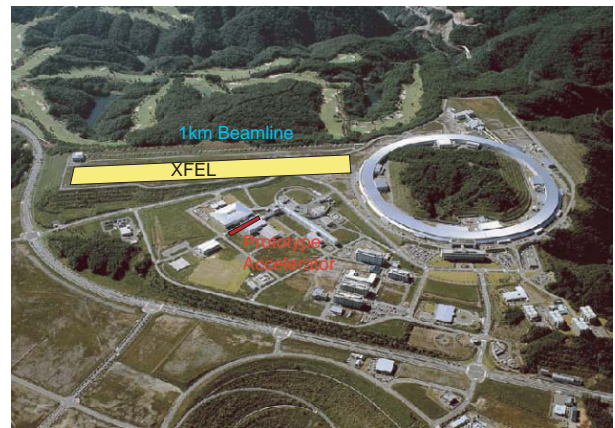

Figure 1: Photograph of the SPring-8 facility and a building site for the XFEL facility (planned). The prototype accelerator is now under construction in the existing building painted red.

Table 1: Example of a magnetic device configuration and focusing force distribution in the undulator line.

Parameter	Prototype	XFEL
Electron Energy (GeV)	0.25	6~8
Normalized Emittance (πmm.mrad)	1.0	0.85
Energy Spread (10^{-4})	2	1
Peak Current (A)	300	3000
Undulator Period (mm)		15
Undulator Length (m)		4.5
Undulator K Value		1.3
Undulator Gap (mm)		3.5
Wavelength (nm)	60	0.1
Gain Length (m)	0.31	3.6
Saturation Length (m)	6.6	68

250-MEV PROTOTYPE ACCELERATOR

Although the facility scale of the prototype accelerator is much smaller than the XFEL facility under proposal, it is composed of essential accelerator components that have
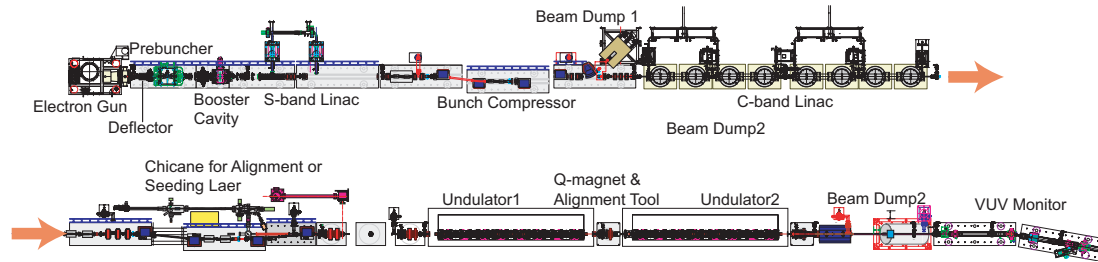

Figure 2: Example of a magnetic device configuration and focusing force distribution in the undulator line.

been developed for the XFEL facility. An overall layout of the prototype accelerator is shown in Fig. 2. A low-emittance electron beam is generated by a thermionic-cathode gun driven by a pulsed DC voltage, accelerated by high-gradient C-band accelerator cavity, and injected to short-period in-vacuum undulators. Thus, the prototype accelerator not only examines feasibility of each accelerator component but also helps us to have perspective of construction and operation of the XFEL facility. In addition, technologies essential for realization of the XFEL, such as the alignment schemes of the BPMs and how to generate and distribute a reference timing signal for the accelerator and FEL beamlines can be tested in the prototype accelerator. A seeding scheme at 60nm will be also tested using high harmonic of a Ti:Sa Laser produced in Xe gas [4].

R&DS OF ACCELERATOR COMPONENTS

Most of the accelerator components to be adopted in the SCSS XFEL facility are newly designed and have not yet been used in any actual accelerators. It is therefore necessary to carefully test each component and carry out R&Ds to improve the performance, the results of which are presented in the following sections.

Electron Gun

The electron beam generated by the electron gun should have a good quality (high peak current and low emittance) to achieve saturation of the FEL radiation power. Moreover, it should be stable enough for long periods from the application point of view. To meet such a requirement, we have decided to use a thermionic cathode followed by a buncher system [6]-[9].

As a cathode material, we have chosen CeB_6, which can emit an intense current over long lifetimes. In practice, single crystal CeB_6 cathodes are widely used for electron microscopy.

A prototype electron gun has been constructed (Fig. 3) and tested with a pulsed voltage of 500 kV applied to obtain a peak current of 1 A. The beam emittance was measured with a double-slit system combined with CT monitors, and an emittance of 1.1πmm.mrad was obtained. If was veri-

Figure 3: Prototype of an electron gun for SCSS.

fied that an emittance of 0.6πmm.mrad could be achieved if a nonlinear tail brought by a space charge effect was eliminated.

Injector and Bunch Compressor

In order to form a nsec single bunch from the long pulse generated by the pulsed DC gun, a beam deflector with a fast pulser has been exploited. A 238 MHz sub-harmonic buncher followed by a 1.6 m drift section and a 476 MHz booster cavity compress the electron bunch by adiabatic bunching. One (prototype) or two (XFEL) bunch compressors are used to obtain a high peak current necessary for saturation.

Start-to-end simulations have been carried out [10] to look for an optimum set of RF phases and bunch compressor configurations. The initial electron distribution in the phase space was reconstructed from the emittance measurements and used for the simulation. The results are shown in Fig. 4 for the prototype and XFEL facilities.

C-band High Gradient Test

C-band (5712 MHz) choke-mode type accelerating structure will be used for the main accelerator [11]-[12]. High-gradient test of a prototype accelerating cavity has been carried out [13]-[14]. The experimental setup is
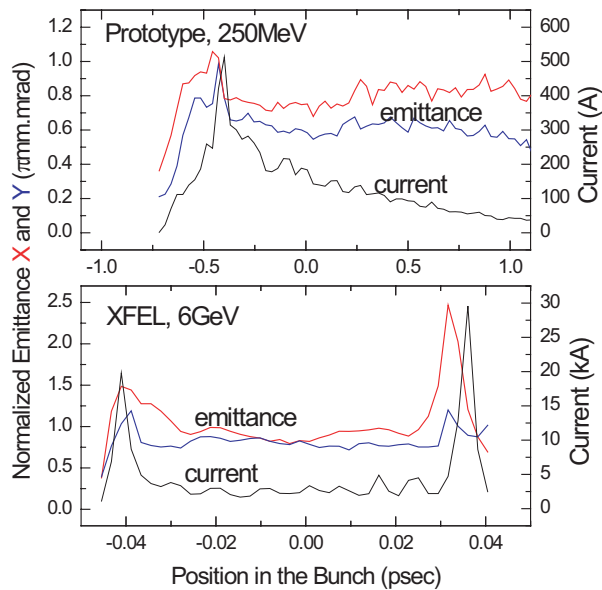
Figure 4: Results of start-to-end simulations for the injector and bunch compressor in the prototype accelerator and XFEL facility.

shown in Fig. 5. An accelerating gradient of up to 33 MV/m was obtained at 55 MW rf peak power, after 344-hour rf processing. During operation, no difficulty was found even at the gradient of 32 MV/m. We also confirmed that rf parameters (attenuation, filling time, etc.) has achieved design values and no phase shift was observed during operation, which means the structure suffered no damage. Amount of dark current generated by rf is 89 pC for each pulse at 32 MV/m and 700 nsec pulse width. A dark current profile shows that most of the dark current started edges around the beam holes and it did not travel along the beam axis.

Figure 5: C-band accelerator setup for high-gradient test.

Ceramic Support Stand

A stable ceramic stand has been developed (Fig. 6) in order to support high-precision BPMs. It is made from "cordierite" with a very low thermal expansion coefficient of $\sim 2 \times 10^{-6}$/K [15]-[16], which is about ten times lower than that of steel, thus provides higher stability against temperature variation. Additionally, position adjustment screws were removed from supporting structure design, i.e., the ceramic stand will be directly placed on a very flat concrete floor, which is polished by a special grinding machine, and accelerator components will be directly mounted on the top flange of the stand without using level adjustment screws.
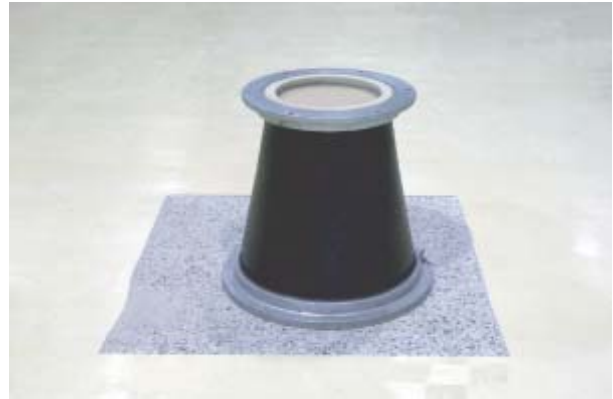

Figure 6: Ceramic stand to support accelerator components such as the BPMs, quadrupole magnets, C-band accelerating tube.

In-vacuum Undulator

Because of the short length of the magnetic period, a very narrow gap is needed to obtain sufficient magnetic field strength. An in-vacuum structure where the magnetic arrays are placed inside the vacuum chamber can provide a narrower gap than the conventional outside-vacuum structure, because there is no vacuum chamber between the magnet gaps. Such a configuration is also important for SCSS project that a wide vertical aperture (25 mm) can be realized by fully opening the magnet gap. This will help with the initial commissioning of the electron beam and alignment of BPMs using an optical laser. A prototype in-vacuum undulator has been constructed as shown in Fig. 7. In spite of a large number of periods (300), a good field performance, i.e., 2.76-degree phase error, has been achieved after a field-correction procedure [17]. An FEL simulation code has been developed that can take into account the effects due to the undulator field error [18], and it was found that magnetic performance of the constructed undulator was close to ideal.

Laser Alignment

In order to ensure an FEL gain over a long distance of the undulator line, the electron trajectory should be as straight as possible, meaning that the BPMs should be well aligned. The tolerance of the BPM alignment has been studied nu-

Figure 7: In-vacuum undulator for SCSS project.

merically and analytically [19] to find the tolerance of several micron. To meet such a requirement, the BPMs will be aligned with a HeNe laser beam introduced in the same line as the electron beam. The in-vacuum undulator has the full gap of 25 mm, which is enough to transport the HeNe laser beam for a long distance. An alignment iris that has the same mechanical origin as the cavity-type BPM is inserted to generate a diffraction image on the CCD camera downstream, which is used to measure the position of the BPM. In order to demonstrate feasibility of the alignment procedure, we made experimental setup in air with vinyl tunnel shield and measured laser spot with the iris being moved along the horizontal axis. We have found that the center of the laser spot reproduced the mechanical movement of the iris with an accuracy better than 1μm.
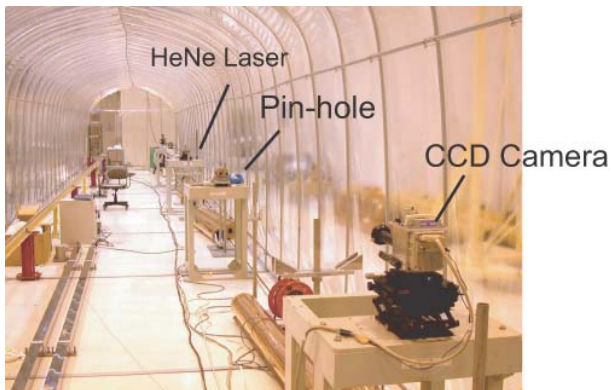

Figure 8: Experimental setup for investigation of the alignment scheme using diffraction pattern.

TIME SCHEDULE OF THE PROTOTYPE ACCELERATOR

Construction of the building for the prototype accelerator has been completed and the accelerator components are now being installed in the accelerator tunnel. From October 2005, RF aging will be started together with final check of operation of all the components. The beam commissioning will be started from November, and the first light is expected to be observed by the end of November.

ACKNOWLEDGEMENTS

REFERENCES

[1] T. Shintake, H. Matsumoto, T. Ishikawa and H. Kitamura, Proc. SPIE2001.

[2] T. Shintake, Proc. APAC2004.

[3] T. Shintake, T. Tanaka, T. Hara, K. Togawa, T. Inagaki, Y. J. Kim, T. Ishikawa, H. Kitamura, H. Baba, H. Matsumoto, Shigeru Takeda, M. Yoshida and Y. Takasu, Nucl. Instrum. Meth. A507 (2003) 382.

[4] G. Lambert, M. Bougeard, W. Boutu, P. Breger, M. E. Couprie, D. Garzella, H. Merdji, P. Monchicourt, P. Salieres, B. Carre, T. Hara, H. Kitamura, T. Shintake, these proceedings.

[5] T. Shintake, H. Kitamura and T. Ishikawa, Proc. SRI2003.

[6] K. Togawa, H. Baba, K. Onoe, T. Shintake, and T. Ishizuka, Proc. PAC2003.

[7] K. Togawa, H. Baba, K. Onoe, T. Inagaki, T. Shintake and H. Matsumoto, Nucl. Instrum. Meth. A528 (2004) 312.

[8] K. Togawa, T. Tanaka, K. Onoe, T. Inagaki, H. Baba, T. Shintake and T. Ohata, Proc. APAC2004.

[9] K. Togawa, T. Shintake, H. Baba, T. Inagaki, K. Onoe, T. Tanaka, and H. Matsumoto, Proc. LINAC2004.

[10] T. Hara, H. Kitamura, T. Shintake, Proc. FEL2004.

[11] H. Matsumoto, S. Takeda, T. Shintake, H. Baba, T. Inagaki, Y. J. Kim, K. Togawa, and H. Kitamura, Proc. LINAC2002

[12] T. Inagaki, H. Baba, T. Shintake, K. Shirasawa, Proc. of IEEE Pulsed Power Conf (2005)

[13] T. Inagaki, T. Shintake, H. Baba, K. Togawa, K. Onoe, X. Marechal, T. Takashima, S. Takahashi and H. Matsumoto Proc. of 1st Accel. Society of Japan (2004) (in Japanese)

[14] T. Inagaki, K. Onoe, T. Shintake, H. Baba, X. Marechal, S. Takahashi, H. Matsumoto and S. Miura, Proc. of 2nd Accel. Society of Japan (2005) (in Japanese).

[15] T. Saeki, T. Shintake, N. Hoshijima, M. Yoshioka, K. Miura and K. Nakaushiro, Proc. APAC2004.

[16] Y. Otake, T. Shintake, T. Seike and K. Nakaushiro, Proc. 2nd Accel. Society of Japan (2005) (in Japanese).

[17] T. Tanaka, K. Shirasawa, T. Seike and H. Kitamura, Proc. SRI2003.

[18] T. Tanaka, Proc. FEL2004.

[19] T. Tanaka, H. Kitamura and T. Shintake, Nucl. Instrum. Meth. A528 (2004) 172.